Forward-looking portfolio selection with multivariate non-Gaussian models

Published Version:
Bianchi M.L., Tassinari G.L. (2020). Forward-looking portfolio selection with multivariate non-Gaussian models. QUANTITATIVE FINANCE, 20(10), 1645-1661 [10.1080/14697688.2020.1733057].

Availability:
This version is available at: https://hdl.handle.net/11585/945254 since: 2023-10-16

Published:

DOI: http://doi.org/10.1080/14697688.2020.1733057

Forward-looking portfolio selection with multivariate non-Gaussian models

Michele Leonardo Bianchi[a,*], Gian Luca Tassinari[b]

[a] *Regulation and Macroprudential Analysis Directorate, Bank of Italy,*
Via Milano 53, 00184, Rome, Italy
micheleleonardo.bianchi@bancaditalia.it
[*] Corresponding author

[b] *Department of Economics, Department of Statistical Sciences "Paolo Fortunati",*
and Department of Management, University of Bologna
Piazza Scaravilli, 2, 40126 Bologna, Italy
gianluca.tassinari2@unibo.it

This version: February 18, 2020

Abstract. In this study we suggest a portfolio selection framework based on time series of stock log-returns, option-implied information, and multivariate non-Gaussian processes. We empirically assess a multivariate extension of the normal tempered stable (NTS) model and of the generalized hyperbolic (GH) one by implementing an estimation method that simultaneously calibrates the multivariate time series of log-returns and, for each margin, the univariate observed one-month implied volatility smile. To extract option-implied information, the connection between the historical measure P and the risk-neutral measure Q, needed to price options, is provided by the multivariate Esscher transform. The method is applied to fit a 50-dimensional series of stock returns, to evaluate widely-known portfolio risk measures and to perform a forward-looking portfolio selection analysis. The proposed models are able to produce asymmetries, heavy tails, both linear and non-linear dependence and, to calibrate them, there is no need of liquid multivariate derivative quotes.

Keywords: normal mean-variance mixtures, time-changed Brownian motion, multivariate non-Gaussian processes, portfolio risk measures, portfolio optimization.

JEL: C13, C22, C63.

Acknowledgments. The authors wish to acknowledge the helpful suggestions of two anonymous referees. The views expressed in this article are those of the authors, and do not necessarily reflect those of the Bank of Italy.

1 Introduction

A portfolio selection problem is by its nature a multi-dimensional problem, and it is usually investigated by considering a multivariate Gaussian model for the description of assets log-returns. The complexity of the problem increases if one moves from a normal distributional assumption to a non-normal one. Additionally, if one wants to define a multivariate non-Gaussian option pricing model, the complexity increases further because the asset return dynamics specified under the *historical* (or *physical*) measure P cannot be directly used to price options, and a *risk-neutral* measure Q cannot, in general, be specified by simply mean-correcting the physical process. Implied volatilities extracted from option prices contain information about the future behavior of asset returns and for this reason they should be considered in portfolio selection (see DeMiguel et al. [2013] and Kempf et al. [2015]). As observed by Cecchetti and Sigalotti [2013], risk-neutral distributions extracted from option prices reflect market participant expectations and, accordingly, they are inherently *forward-looking*. Thus, risk-neutral information may provide more accurate estimates of risk factors distribution and related moments, and they can be used to infer market beliefs about economic events of interest both in portfolio management, where they can be used in portfolio selection, and in central banks, where they are routinely used for monetary policy and financial stability purposes (see Taboga [2016]).

In this paper we propose a portfolio selection framework that takes into account time series of stock log-returns, option-implied information and multivariate non-Gaussian processes. We empirically assess a multivariate extension of the normal tempered stable (NTS) model and the generalized hyperbolic (GH) one. More precisely, we improve and extend the works of Tassinari and Bianchi [2014] and Bianchi et al. [2016] under different perspectives: (1) we discuss the change of measure problem for multivariate GH and multivariate NTS models; (2) we conduct a large scale estimation that considers stock log-returns and option-implied information; and (3) we apply the estimated models to perform an effective forward-looking portfolio selection analysis. In this paper we start with theoretical models and then we explore the way to turn them into a potential portfolio selection strategy.

The multivariate normal tempered stable (MNTS) and the multivariate generalized hyperbolic (MGH) distributions are generalizations of the multivariate normal distribution known as multivariate normal mean-variance mixtures. These distributions can be viewed as an enhancement of the multivariate normal distribution allowing for asymmetries, heavy tails, and both linear and non-linear dependence. According to Frahm [2004], both the MNTS and the MGH distributions belong to the class of elliptical variance-mean mixture. Elliptical and generalized elliptical heavy tail distributions have been discussed, for example, by Kring et al. [2009], Dominicy et al. [2013], Zhou et al. [2014], and Fallahgoul et al. [2016]. The MNTS has been introduced by Kim et al. [2012] and extensively studied by Bianchi et al. [2016], Fallahgoul et al. [2019] and Bianchi et al. [2019]. The MGH is a popular choice when deviating from the multivariate normal distribution towards fatter tailed multivariate distributions (see Protassov [2004], Hu [2005], McNeil et al. [2005], Hu and Kercheval [2007], and Hu and Kercheval [2010], Hellmich and Kassberger [2011]). From a dynamic perspective, the MNTS and the MGH processes are more general Lévy processes than the multivariate arithmetic Brownian motion. These processes are known as time-changed Brownian motions.

In non-Gaussian continuous-time models, given a historical measure P, the change of measure needed to price options is not unique. This means that to find a proper risk-neutral measure Q it is necessary to estimate the model by also considering the quotes of options traded in the market. In this study the change of measure between the historical measure P and the risk-neutral measure Q is given by the Esscher transform (see Gerber and Shiu [1994], Sato [1999], Tassinari and Corradi [2013], Tassinari and Corradi [2014], and Tassinari and Bianchi [2014]). We discuss a possible approach to jointly estimate multivariate asset log-returns under the historical measure and calibrate, for each margin, option implied volatilities under the risk-neutral measure. Tassinari and Bianchi [2014] proposed a joint calibration-estimation of the univariate option surfaces (one surface for each margin) and of the multivariate time series of log-returns by considering the EM-based maximum likelihood estimation method together with the multivariate Esscher transform applied to find the link between historical and risk-neutral parameters. The authors have referred to this joint calibration-estimation as *double calibration*. A similar calibration procedure which rests on a joint calibration of univariate option surfaces and pairwise correlations has been introduced by Guillaume [2012] and Guillaume [2013]. Recently, Ballotta et al. [2017] proposed a joint calibration to market quotes for both FX triangles and quanto products. In this paper we apply the double calibration approach to the MNTS and MGH case by considering the same dataset of Tassinari and Bianchi [2014]. Then, we assess the same calibration procedure to fit both the MGH and the MNTS models on all Euro denominated stocks included in the EuroStoxx 50. In this second empirical application, the models are fitted on the time series of stock log-returns and on the 50 one-month implied volatility smiles. As observed by Carr et al. [2007] and Guillaume [2012], Lévy processes are suited to replicate option prices for one single maturity, but are generally not able to reproduce quoted univariate option prices in both the strike and time-to-maturity dimensions (i.e. for the whole set of quoted maturities) with sufficient precision, particularly during investor fear periods.

Most of the papers on multivariate models of stock log-returns are mainly theoretical (e.g. Luciano and Semeraro [2010]) or conduct empirical studies on few assets (e.g. four in Hellmich and Kassberger [2011], five in Hu and Kercheval [2010]) with some exceptions (ten in Luciano et al. [2016] and 20 in Fallahgoul et al. [2016]). We conduct a large scale empirical application and show that with 50 stocks our models work properly (at least for the data considered in this study). Furthermore, the multivariate non-Gaussian models mentioned above are estimated by considering historical information only. The main advantage of our approach is that our estimates are based on both historical and risk-neutral information. Additionally, our approach can also be used in the pricing of multivariate derivative contracts. In most of the papers on multivariate non-Gaussian option pricing models, a multivariate stochastic process is calibrated using a limited number of assets (e.g. three in Ballotta and Bonfiglioli [2016] and four in Guillaume [2013]). The margins are calibrated using univariate options quotes and the parameters characterizing the joint distribution are estimated by minimizing the distance between the empirical and theoretical correlation matrix. The so called mean-correcting martingale method is applied to price derivatives (see Schoutens [2003]), that is only the mean of the physical process is changed to ensure that the discounted price process of every assets is a martingale under the pricing measure, all other moments, co-moments, and parameters are left unchanged and the historical correlation matrix can be used to calibrate the risk-neutral one. The models described in this paper are based on the Esscher transform that allows one to properly combine risk-neutral and historical information.

After having defined the multivariate model, we consider a minimum-risk portfolio selection approach. The risk measure we select is the average value at risk (AVaR), the average of the values-at-risk (VaRs) greater than the VaR at a given tail level. AVaR, also called conditional value-at-risk (CVaR) or expected shortfall, is a superior risk measure to VaR because it satisfies all axioms of a coherent risk measure and it is consistent with preference relations of risk-averse investors (see Rachev et al. [2008]). Thus, we follow a mean-AVaR portfolio selection criterion which, by construction, not only takes into consideration the first two moments of the log-returns distribution but also the heaviness of its left tail. In the models we propose, the AVaR has a closed formula (up to a numerical integration), which can be easily cast into a portfolio optimization problem. In the empirical analysis we consider minimum-AVaR (MA) portfolios (see Stoyanov et al. [2010]) under the normal, the MNTS and the MGH distributional assumption, respectively, and, as done in similar studies (e.g. DeMiguel et al. [2007] and Mainik et al. [2015]), we compare them with two benchmark portfolios: the minimum-variance portfolio (MV) and the equally weighed portfolio (EW). Then, as robustness check, we perform a portfolio selection analysis by maximizing the portfolio expected return under different levels of risk, where the risk is measured by the portfolio AVaR.

The paper is organized as follows. In Sections 2.1 and 2.2, we introduce the MNTS model and the MGH one, respectively. For both models we also show how to get the risk-neutral parameters knowing the historical ones through the multivariate Esscher transform, and how to find the historical parameters knowing the risk-neutral ones by means of the inverse Esscher transform. In Section 3, we briefly describe the data analyzed in the empirical study and, in Section 4, after having reviewed the double calibration algorithm, we compare the calibration errors of both the MGH and the MNTS models with those reported in Tassinari and Bianchi [2014], that is, with the ones of the multivariate Gaussian, the multivariate variance gamma (MVG) and the multivariate normal inverse Gaussian (MNIG) models, and we conduct a large scale empirical test on a 50-dimensional series of stock returns. In Section 5, after having explained the minimum-AVaR portfolio selection approach, we describe the main computational aspects of our forward-looking approach and we discuss the results. Section 6 resumes the main contributions of the paper and contains the conclusions.

2 Time-changed Brownian motion

In this section we review the model described in Tassinari and Bianchi [2014]. Consider a market with n equities, with continuous dividend yields $d = [d_j]_{n\times 1}$, and one riskless asset, which guarantees a constant continuously compounded rate of return r. The evolution of equity log-returns is driven by a multivariate generalized Brownian motion, with correlated components, stochastically time-changed by an independent univariate subordinator. Formally, the log-returns process $Y = \{Y_t, t \geq 0\}$ is defined as

$$Y_t = \mu t + \theta S_t + D_\sigma W_{S_t}, \tag{2.1}$$

where

- $W = \{W_t, t \geq 0\}$ is an n-dimensional Brownian motion with correlation matrix $\Omega = [\rho_{jk}]_{n \times n}$;
- $S = \{S_t, t \geq 0\}$ is a *one*-dimensional subordinator independent of W, with Laplace exponent $l_{S_1}(.)$;
- $W_S = \{W_{S_t}, t \geq 0\}$ is the Brownian motion W time-changed with the subordinator S;
- D_σ is a diagonal matrix having on its main diagonal the elements of the vector $\sigma = [\sigma_j]_{n \times 1} \in \mathbb{R}^n_+$;
- $\mu = [\mu_j]_{n \times 1}$ and $\theta = [\theta_j]_{n \times 1}$ are vectors in $\mathbb{R}^n$.

There exists a relation between subordinated multivariate Brownian motions and multivariate distributions defined as normal mean-variance mixtures. More precisely, for each discrete time step Δt, the distribution of the log-returns is given by

$$Y_{\Delta t} = \mu \Delta t + \theta S_{\Delta t} + \sqrt{S_{\Delta t}} D_\sigma A Z, \tag{2.2}$$

where

- Z is a n-dimensional standard normal random vector with uncorrelated components;
- $S_{\Delta t}$ is the random variable describing the subordinator increments and it is independent of Z;
- A is the lower Cholesky decomposition of the correlation matrix Ω;
- D_σ, μ and θ are the matrix and the vectors defined above.

The representation (2.2) is useful to implement the expectation-maximization (EM) maximum likelihood estimation on the time series of log-returns (see McNeil et al. [2005] and Bianchi et al. [2016]).

As shown in Tassinari and Bianchi [2014], the characteristic function of the log-returns process is given by

$$\Psi_{Y_t}(u) = \exp\left[itu'\mu + tl_{S_1}\left(iu'\theta - \frac{1}{2}u'\Sigma u \right) \right], \tag{2.3}$$

where $\Sigma = D_\sigma \Omega D_\sigma = [\sigma_{jk}]_{n \times n} \in \mathbb{R}^{n \times n}$ and $u = [u_j]_{n \times 1} \in \mathbb{R}^n$.

As already explained, we want to perform a portfolio selection analysis based on the physical log-returns model (2.1) using both time series of stock log-returns and option-implied information. To reach this objective, we implement the double calibration procedure of Tassinari and Bianchi [2014], an estimation method that simultaneously calibrate the multivariate time series of log-returns and, for each of the n stocks, the univariate observed volatility smile. To extract option-implied information, the connection between the historical measure P and the risk-neutral measure Q, needed to price options, is provided by the multivariate Esscher transform. In particular, given the historical parameters, this change of measure allows to get the risk-neutral ones and, conversely, given the risk-neutral ones, through the inverse Esscher transform, it allows to get the historical parameters. Specifically, if one can find a vector $h = [h_j]_{n\times 1} \in \mathbb{R}^n$ solving the system

$$\ln \Psi_{Y_1}\left(-ih_{(j)}\right) - \ln \Psi_{Y_1}(-ih) = r - d_j, \quad j = 1, 2, ...n, \tag{2.4}$$

where $h_{(j)} = [h_1, ..., h_{j-1}, h_j + 1, h_{j+1}, ..., h_n]'$, then the Esscher equivalent martingale measure exists and the characteristic function of the log-returns process under the risk-neutral probability Q_h is given by

$$\Psi_{Y_t}^{Q_h}(u) = \Psi_{Y_t}(u - ih) / \Psi_{Y_t}(-ih). \tag{2.5}$$

On the other hand, given the risk-neutral parameters, the inverse Esscher transform allows to get the physical ones, by finding the vector h that solves the system

$$\ln \Psi_{Y_1^j}^{Q}(-i) = r - d_j, \quad j = 1, 2, ..., n, \tag{2.6}$$

with the additional constraints on the relations between historical and risk-neutral parameters that are obtained from the comparison between (2.5) and (2.3) for each specific model. This procedure is extensively explained in Tassinari and Bianchi [2014] and applied to the multivariate variance gamma (MVG) and to the multivariate normal inverse Gaussian (MNIG) models. In this paper we extend the framework to the MNTS and the MGH models.

2.1 The multivariate NTS model

The tempered stable family was introduced by Barndorff-Nielsen [1997], Barndorff-Nielsen and Levendorskii [2001], Boyarchenko and Levendorskii(2000, 2002) from both a univariate and multivariate perspective, further studied on a theoretical level by Rosinski [2007], Bianchi et al. [2010] and Grabchak [2016] and applied to finance in numerous empirical studies principally under a univariate framework (see Carr et al. [2002], Cont and Tankov [2003], Kim et al. [2010a], Rachev et al. [2011], Bianchi [2015] and references therein). In this section we study the multivariate extension of the normal tempered stable model proposed by Kim et al. [2012] and extensively studied by Bianchi et al. [2016], Anand et al. [2016], Fallahgoul et al. [2019] and Bianchi et al. [2019]. Let $S = \{S_t,\ t \geq 0\}$ be a classical tempered stable process, that is, a process which starts at zero and has stationary and independent increments, in which the law of S_1 is classical tempered stable (CTS) with parameters $\lambda > 0$, $C > 0$ and $0 < \alpha < 2$. We refer to the law S_1 as $CTS(\alpha, \lambda, C)$. The characteristic function of the random variable S_1 is

$$\Psi_{S_1}(v) = \exp\left[C\Gamma(-\alpha)((\lambda - iv)^\alpha - \lambda^\alpha))\right]. \tag{2.7}$$

From (2.7) it is possible to derive the Laplace exponent of the classical tempered stable subordinator

$$l_{S_1}(v) = \ln \Psi_{I_1}\left(\frac{v}{i}\right) = C\Gamma(-\alpha)((\lambda - v)^\alpha - \lambda^\alpha),$$

and the main moments of S_1

$$E[S_1] = -\alpha C\Gamma(-\alpha)\lambda^{\alpha-1},$$

$$var\,[S_1] = \alpha(\alpha-1)C\Gamma(-\alpha)\lambda^{\alpha-2},$$
$$skew\,[S_1] = (2-\alpha)\left[\alpha(\alpha-1)C\Gamma(-\alpha)\lambda^{\alpha}\right]^{-\frac{1}{2}},$$
$$kurt\,[S_1] = 3 + (\alpha-2)(\alpha-3)\left[\alpha(\alpha-1)C\Gamma(-\alpha)\lambda^{\alpha}\right]^{-1}.$$

Using (2.1), we obtain the characteristic function of the multivariate normal tempered stable (MNTS) process

$$\Psi_{Y_t}(u) = \exp\left\{t\left[iu'\mu + C\Gamma(-\alpha)\left(\left(\lambda - iu'\theta + \frac{1}{2}u'\Sigma u\right)^{\alpha} - \lambda^{\alpha}\right)\right]\right\}. \tag{2.8}$$

If we set $\alpha = 1/2$, S_1 follows an inverse Gaussian distribution with parameters $\gamma = -\frac{C\Gamma(-\alpha)}{\sqrt{2}}$ and $\eta = \sqrt{2\lambda}$. If $\alpha \to 0$, S_1 follows a gamma distribution with parameters $\alpha' = -\frac{C\Gamma(-\alpha)}{\sqrt{2}}$ and $\beta' = \sqrt{2\lambda}$. In the first case, the MNTS model becomes the multivariate normal inverse Gaussian (MNIG) and, in the second case, the multivariate variance gamma (MVG) considered in Tassinari and Bianchi [2014].

Using (2.8), the log-returns moments can be derived

$$E\left[Y_t^j\right] = \mu_j t + E\left[S_t\right]\theta_j,$$
$$var\left[Y_t^j\right] = var\left[S_t\right]\left(\theta_j^2 + \frac{\sigma_j^2\lambda}{1-\alpha}\right),$$
$$skew\left[Y_t^j\right] = skew\left[S_t\right]\left(\theta_j^3 + \frac{3\theta_j\sigma_j^2\lambda}{2-\alpha}\right)\left(\theta_j^2 + \frac{\sigma_j^2\lambda}{1-\alpha}\right)^{-\frac{3}{2}},$$
$$kurt\left[Y_t^j\right] = 3 + \left(kurt\left[S_t\right]-3\right)\left[\theta_j^4 + \frac{3\sigma_j^2\lambda}{3-\alpha}\left(2\theta_j^2 + \frac{\sigma_j^2\lambda}{2-\alpha}\right)\right]\left(\theta_j^2 + \frac{\sigma_j^2\lambda}{1-\alpha}\right)^{-2},$$
$$cov\left[Y_t^j;Y_t^k\right] = var\left[S_t\right]\left(\theta_j\theta_k + \frac{\sigma_{kj}\lambda}{1-\alpha}\right),$$
$$corr\left[Y_t^j;Y_t^k\right] = \frac{\theta_j\theta_k + \frac{\sigma_j\sigma_k\rho_{jk}\lambda}{1-\alpha}}{\sqrt{\left(\theta_j^2 + \frac{\sigma_j^2\lambda}{1-\alpha}\right)\left(\theta_k^2 + \frac{\sigma_k^2\lambda}{1-\alpha}\right)}}, \tag{2.9}$$

where Y_t^j and Y_t^k denote the log-return of the j-th and the k-th stock, respectively, on time intervals of lenght t.

To perform the change of probability measure, we follow the procedure described in Tassinari and Bianchi [2014]. By considering equations (2.4) and (2.8), to find the vector h we need to solve the following system

$$\begin{cases} (\lambda - l(h))^{\alpha} - \left(\lambda - \theta_1 - \frac{1}{2}\sigma_1^2 - l(h) - \sum_{j=1}^{n} h_j\sigma_1\sigma_j\rho_{1j}\right)^{\alpha} & = (\mu_1 + d_1 - r)/C\Gamma(-\alpha) \\ & \vdots \\ (\lambda - l(h))^{\alpha} - \left(\lambda - \theta_n - \frac{1}{2}\sigma_n^2 - l(h) - \sum_{j=1}^{n} h_n\sigma_n\sigma_j\rho_{nj}\right)^{\alpha} & = (\mu_n + d_n - r)/C\Gamma(-\alpha), \end{cases} \tag{2.10}$$

where

$$l(h) = h'\theta + \frac{1}{2}h'\Sigma h.$$

Although it is difficult to prove the existence of a solution, in all of our applications we were able to find it through numerical methods. This ensures that at least an equivalent risk-neutral measure exists.

Using equation (2.5), we get the characteristic function under the risk-neutral measure Q_h

$$\Psi_{Y_t}(u) = \exp\left\{ t \left[iu'\mu^{Q_h} + C^{Q_h}\Gamma\left(-\alpha^{Q_h}\right) \left(\left(\lambda^{Q_h} - iu'\theta^{Q_h} + \frac{1}{2}u'\Sigma^{Q_h}u \right)^{\alpha^{Q_h}} - {\lambda^{Q_h}}^{\alpha^{Q_h}} \right) \right] \right\}, \tag{2.11}$$

where

$$\begin{aligned} \mu^{Q_h} &= \mu, \\ C^{Q_h} &= C, \\ \alpha^{Q_h} &= \alpha, \\ \lambda^{Q_h} &= \lambda - h'\theta - \frac{1}{2}h'\Sigma h, \\ \theta^{Q_h} &= \theta + \Sigma h, \\ D_{\sigma^{Q_h}} &= D_\sigma, \\ \alpha^{Q_h} &= \alpha. \end{aligned} \tag{2.12}$$

By comparing (2.8) with (2.11), it is evident that the risk-neutral log-returns dynamics is still described by a MNTS process. The Esscher change of measure modifies only the parameter λ and the vector θ. Even if the correlation matrix of the underlying Brownian motion is not affected by the change of measure, the historical and risk-neutral correlations are different (see (2.9) and (2.12)). Furthermore, all risk-neutral marginal moments differ from the historical ones since they depend on the whole historical dependence structure. More precisely, the risk-neutral moments of each margin are a function of all the elements of the vector θ and the matrix Σ through the vector h, which in turn depends on the joint physical log-returns process.

The inverse Esscher transform allows one to find the parameters under the physical measure P_h starting from the ones under the risk-neutral measure Q. By considering equations (2.6) and (2.12), it follows that to find h the following system has to be solved

$$\begin{cases} \mu_1^Q + C^Q\Gamma\left(-\alpha^Q\right)\left(\left(\lambda^Q - \theta_1^Q - \frac{1}{2}{\sigma_1^Q}^2\right)^{\alpha^Q} - {\lambda^Q}^{\alpha^Q}\right) = r - d_1 \\ \vdots \\ \mu_n^Q + C^Q\Gamma\left(-\alpha^Q\right)\left(\left(\lambda^Q - \theta_n^Q - \frac{1}{2}{\sigma_n^Q}^2\right)^{\alpha^Q} - {\lambda^Q}^{\alpha^Q}\right) = r - d_n \\ \mu^{P_h} = \mu^Q \\ C^{P_h} = C^Q \\ \alpha^{P_h} = \alpha^Q \\ \lambda^{P_h} = \lambda^Q + h'\theta^Q - \frac{1}{2}h'\Sigma^Q h \\ \theta^{P_h} = \theta^Q - \Sigma^Q h \\ D_{\sigma^{P_h}} = D_{\sigma^Q} \\ \alpha^{P_h} = \alpha^Q. \end{cases} \tag{2.13}$$

Since the system must satisfy the constraints in (2.12), the unknowns to be found are the vector h together with the parameters λ^{P_h} and θ^{P_h}.

2.2 The multivariate GH model

The generalize hyperbolic (GH) distribution has received a lot of attention in the financial-modeling literature (see for example Eberlein and Keller [1995], Prause [1999], and Eberlein et al. [2002]). The GH parametric family includes many familiar distributions such as for example the Student's t, the skew-t, the hyperbolic, the variance gamma, and the normal inverse Gaussian. In this section we study the multivariate generalized hyperbolic (MGH) distribution. Let $G = \{G_t,\ t \geq 0\}$ be a generalized inverse Gaussian process (GIG), i.e., a process which starts at zero and has stationary and independent increments, in which the distribution of G_1 is generalized inverse Gaussian with parameters ϵ, ψ, χ. ψ and χ are are both nonnegative and not simultaneously 0. We refer to the law of G_1 as GIG (ϵ, χ, ψ). The density function of the random variable G_1 is

$$f(x; \epsilon, \psi, \chi) = \frac{1}{2K_\epsilon\left(\sqrt{\chi\psi}\right)}\left(\frac{\psi}{\chi}\right)^{\frac{\epsilon}{2}} x^{\epsilon-1}\exp\left[-\frac{1}{2}\left(\frac{\chi}{x} + \psi x\right)\right], x > 0, \tag{2.14}$$

and its characteristic function is

$$\Psi_{G_1}(v) = \left(1 - \frac{2iv}{\psi}\right)^{-\frac{\epsilon}{2}} \frac{K_\epsilon\left(\sqrt{\chi(\psi - 2iv)}\right)}{K_\epsilon\left(\sqrt{\chi\psi}\right)}. \tag{2.15}$$

From (2.15) it is possible to derive the Laplace exponent of the generalized inverse Gaussian subordinator

$$l(v) = \ln \Psi_{G_1}\left(\frac{v}{i}\right) = -\frac{\epsilon}{2}\ln\left(1 - \frac{2v}{\psi}\right) + \ln\frac{K_\epsilon\left(\sqrt{\chi(\psi - 2iv)}\right)}{K_\epsilon\left(\sqrt{\chi\psi}\right)}, \tag{2.16}$$

and from (2.16) the cumulants of G_1

$$c_1\left[G_1\right] = E\left[G_1\right] = \left(\frac{\chi}{\psi}\right)^{\frac{1}{2}} \frac{K_{\epsilon+1}\left(\sqrt{\chi\psi}\right)}{K_\epsilon\left(\sqrt{\chi\psi}\right)},$$

$$c_2\left[G_1\right] = var\left[G_1\right] = \left(\frac{\chi}{\psi}\right)\left[\frac{K_{\epsilon+2}\left(\sqrt{\chi\psi}\right)}{K_\epsilon\left(\sqrt{\chi\psi}\right)} - \left(\frac{K_{\epsilon+1}\left(\sqrt{\chi\psi}\right)}{K_\epsilon\left(\sqrt{\chi\psi}\right)}\right)^2\right],$$

$$c_3\left[G_1\right] = \left(\frac{\chi}{\psi}\right)^{\frac{3}{2}}\left[\frac{K_{\epsilon+3}\left(\sqrt{\chi\psi}\right)}{K_\epsilon\left(\sqrt{\chi\psi}\right)} - \frac{3K_{\epsilon+2}\left(\sqrt{\chi\psi}\right)K_{\epsilon+1}\left(\sqrt{\chi\psi}\right)}{K_\epsilon^2\left(\sqrt{\chi\psi}\right)} + 2\left(\frac{K_{\epsilon+1}\left(\sqrt{\chi\psi}\right)}{K_\epsilon\left(\sqrt{\chi\psi}\right)}\right)^3\right],$$

$$c_4\left[G_1\right] = \left(\frac{\chi}{\psi}\right)^2\left[\frac{K_{\epsilon+4}\left(\sqrt{\chi\psi}\right)}{K_\epsilon\left(\sqrt{\chi\psi}\right)} - \frac{4K_{\epsilon+3}\left(\sqrt{\chi\psi}\right)K_{\epsilon+1}\left(\sqrt{\chi\psi}\right)}{K_\epsilon^2\left(\sqrt{\chi\psi}\right)} - 3\left(\frac{K_{\epsilon+2}\left(\sqrt{\chi\psi}\right)}{K_\epsilon\left(\sqrt{\chi\psi}\right)}\right)^2\right] +$$
$$+ 6\left(\frac{\chi}{\psi}\right)^2\left[\frac{2K_{\epsilon+2}\left(\sqrt{\chi\psi}\right)K_{\epsilon+1}^2\left(\sqrt{\chi\psi}\right)}{K_\epsilon^3\left(\sqrt{\chi\psi}\right)} - \left(\frac{K_{\epsilon+1}\left(\sqrt{\chi\psi}\right)}{K_\epsilon\left(\sqrt{\chi\psi}\right)}\right)^4\right].$$

Using (2.1), we obtain the characteristic function of the multivariate generalized hyperbolic (MGH) process

$$\Psi_{Y_t}(u) = \exp(iu'\mu t)\left[1 - \frac{2}{\psi}\left(iu'\theta - \frac{1}{2}u'\Sigma u\right)\right]^{-\frac{\epsilon t}{2}} \left(\frac{K_\epsilon\left(\sqrt{\chi\left(\psi - 2\left(iu'\theta - \frac{1}{2}u'\Sigma u\right)\right)}\right)}{K_\epsilon\left(\sqrt{\chi\psi}\right)}\right)^t. \tag{2.17}$$

If we set $\epsilon = -1/2$, G_1 follows an inverse Gaussian distribution with parameters $\gamma = \sqrt{\chi}$ and $\eta = \sqrt{\psi}$. If we set $\chi = 0$, G_1 follows a gamma distribution with $\alpha' = \epsilon$ and $\beta' = \psi/2$. In the first case, we get the MNIG model and, in the second one, the MVG analysed by Tassinari and Bianchi [2014].

From equation (2.17), the following marginal and joint moments of the log-returns distribution can be obtained

$$\begin{aligned}
E\left[Y_t^j\right] &= \mu_j t + E\left[G_t\right]\theta_j,\\
var\left[Y_t^j\right] &= E\left[G_t\right]\sigma_j^2 + var\left[G_t\right]\theta_j^2,\\
skew[Y_t^j] &= \frac{c_3[Y_t^j]}{var[Y_t^j]^{3/2}},\\
kurt[Y_t^j] &= 3 + \frac{c_4[Y_t^j]}{var[Y_t^j]^2},\\
cov\left[Y_t^j;Y_t^k\right] &= E\left[G_t\right]\sigma_{jk} + var\left[G_t\right]\theta_j\theta_k,\\
corr\left[Y_t^j;Y_t^k\right] &= \frac{\theta_j\theta_k\Upsilon\sqrt{\chi} + \sqrt{\psi}\sigma_j\sigma_k\rho_{jk}}{\sqrt{\left[\theta_j^2\Upsilon\sqrt{\chi} + \sigma_j^2\sqrt{\psi}\right]\left[\theta_k^2\Upsilon\sqrt{\chi} + \sigma_k^2\sqrt{\psi}\right]}},
\end{aligned} \tag{2.18}$$

where

$$\begin{aligned}
c_3\left[Y_t^j\right] &= 3var\left[G_t\right]\theta_j\sigma_j^2 + c_3\left[G_t\right]\theta_j^3,\\
c_4\left[Y_t^j\right] &= 3var\left[G_t\right]\sigma_j^4 + 6c_3\left[G_t\right]\theta_j\sigma_j^2 + c_4\left[G_t\right]\theta_j^4,
\end{aligned}$$

and

$$\Upsilon = \left(\frac{K_{\lambda+2}\left(\sqrt{\chi\psi}\right)}{K_{\lambda+1}\left(\sqrt{\chi\psi}\right)} - \frac{K_{\lambda+1}\left(\sqrt{\chi\psi}\right)}{K_\lambda\left(\sqrt{\chi\psi}\right)}\right).$$

As observed in Bianchi et al. [2019], in contrast to the MVG, the MNIG and the MNTS cases, assuming that $Y_0 = 0$ by equation (2.15) it follows that if Y_1 is MGH distributed with parameters (λ, χ, ψ, μ, θ, Σ) then the increments $Y_{\Delta t} = Y_{t+\Delta t} - Y_t$ are no longer MGH distributed. This in practice means that for a different time scale we do not know the distribution of the increments but only their characteristic function.

As described in Section (2.1) for the MNTS case, to obtain that the discounted price process of each stock is a martingale under the measure Q^h and, by considering equation

(2.17), the system to solve to find the vector h may be written as

$$\begin{cases} \left[1-\frac{2\left(\theta_1+0.5\sigma_1^2+\sum_{j=1}^n h_j\sigma_{1j}\right)}{\psi-2l(h)}\right]^{-\frac{\epsilon}{2}} \frac{K_\epsilon\left(\sqrt{\chi\left(\psi-2l(h)-2\left(\theta_1+0.5\sigma_1^2+\sum_{j=1}^n h_j\sigma_{1j}\right)\right)}\right)}{K_\epsilon\left(\sqrt{\chi(\psi-2l(h))}\right)} & = \exp(r-\mu_1-d_1) \\ & \vdots \\ \left[1-\frac{2\left(\theta_n+0.5\sigma_n^2+\sum_{j=1}^n h_j\sigma_{nj}\right)}{\psi-2l(h)}\right]^{-\frac{\epsilon}{2}} \frac{K_\epsilon\left(\sqrt{\chi\left(\psi-2l(h)-2\left(\theta_n+0.5\sigma_n^2+\sum_{j=1}^n h_j\sigma_{nj}\right)\right)}\right)}{K_\epsilon\left(\sqrt{\chi(\psi-2l(h))}\right)} & = \exp(r-\mu_n-d_n) \end{cases} \tag{2.19}$$

where

$$l\left(h\right) = h'\theta + \frac{1}{2}h'\Sigma h.$$

As for the system (2.10), a solution for the system (2.19) is found through numerical methods.

By considering equations (2.5) and (2.17), we get the risk-neutral characteristic function

$$\begin{aligned} \Psi_{Y_1}^{Q_h}\left(u\right) = \exp\left(iu'\mu^{Q_h}\right)\left[1-\frac{2}{\psi^{Q_h}}\left(iu'\theta^{Q_h}-\frac{1}{2}u'\Sigma^{Q_h}u\right)\right]^{-\frac{\epsilon^{Q_h}}{2}} \times \\ \frac{K_{\epsilon^{Q_h}}\left(\sqrt{\chi^{Q_h}\left(\psi^{Q_h}-2\left(iu'\theta^{Q_h}-\frac{1}{2}u'\Sigma^{Q_h}u\right)\right)}\right)}{K_{\epsilon^{Q_h}}\left(\sqrt{\chi^{Q_h}\psi^{Q_h}}\right)}, \end{aligned} \tag{2.20}$$

where

$$\begin{aligned} \mu^{Q_h} &= \mu, \\ \chi^{Q_h} &= \chi, \\ \epsilon^{Q_h} &= \epsilon, \\ \psi^{Q_h} &= \psi - 2\left(h'\theta + \frac{1}{2}h'\Sigma h\right), \\ \theta^{Q_h} &= \theta + \Sigma h, \\ D_{\sigma^{Q_h}} &= D_\sigma, \\ \alpha^{Q_h} &= \alpha. \end{aligned} \tag{2.21}$$

Similarly to the MNTS case, by comparing equation (2.17) with equation (2.20), it is evident that the Esscher change of measure does not modify the nature of the log-returns process which is still an MGH one. Only the parameter ψ and the vector θ change. Even if the correlation matrix of the underlying Brownian motion is not affected by the change of measure, the historical and risk-neutral correlations are different (see (2.18) and (2.21)). Finally, observe that all risk-neutral marginal moments differ from the historical ones and they depend on the full physical log-returns process.

To get the parameters under the probability measure P_h, starting from the risk-neutral measure Q, we need to solve the system

$$\begin{cases} \mu_1{}^Q - \frac{\epsilon^Q}{2} \ln\left[1 - \frac{2}{\psi^Q}\left(\theta_1{}^Q + \frac{1}{2}\sigma_1^{Q^2}\right)\right] + \ln \frac{K_{\epsilon^Q}\left(\sqrt{\chi^Q\left(\psi^Q - 2\left(\theta_1{}^Q + \frac{1}{2}\sigma_1^{Q^2}\right)\right)}\right)}{K_{\epsilon^Q}\left(\sqrt{\chi^Q\psi^Q}\right)} = r - d_1 \\ \vdots \\ \mu_n{}^Q - \frac{\epsilon^Q}{2} \ln\left[1 - \frac{2}{\psi^Q}\left(\theta_n{}^Q + \frac{1}{2}\sigma_n^{Q^2}\right)\right] + \ln \frac{K_{\epsilon^Q}\left(\sqrt{\chi^Q\left(\psi^Q - 2\left(\theta_n{}^Q + \frac{1}{2}\sigma_n^{Q^2}\right)\right)}\right)}{K_{\epsilon^Q}\left(\sqrt{\chi^Q\psi^Q}\right)} = r - d_n \\ \mu^{P_h} = \mu^Q, \\ \epsilon^{P_h} = \epsilon^Q \\ \chi^{P_h} = \chi^Q \\ \psi^{P_h} = \psi^Q + 2\left(h'\theta^Q - \frac{1}{2}h'\Sigma^Q h\right) \\ \theta^{P_h} = \theta^Q - \Sigma^Q h \\ D_{\sigma^{P_h}} = D_{\sigma^Q} \\ \alpha^{P_h} = \alpha^Q. \end{cases} \tag{2.22}$$

The system must satisfy the constraints in equation (2.21) and, therefore, the unknowns are the vector h, the parameters ψ^{P_h} and θ^{P_h}.

3 Data

In this section we describe the data used in the empirical analysis. In the first empirical test we consider the same dataset analyzed in Tassinari and Bianchi [2014], that is, daily dividend adjusted closing prices from January 2, 1990 through December 31, 2012 and implied volatilities from January 2, 2008 to December 31, 2012 obtained from Bloomberg for five selected companies included in the S&P 500: Apple Inc. (ticker APPL), Dell Inc. (ticker DELL), International Business Machines Corp. (ticker IBM), Hewlett-Packard Comp. (ticker HPQ), Microsoft Corp. (ticker MSFT). The implied volatilities are extracted from European call and put options with a maturity between one month and one year and with moneyness between 80% and 120%. That dataset is made up of more than 50,000 observations for each company.

Then, for further empirical investigations we use the daily logarithmic return series for all Euro denominated stocks included in the EuroStoxx 50 on April 30, 2017.[1] We obtained from Datastream daily dividend-adjusted closing prices from June 30, 2002 through April 30, 2017. Furthermore, implied volatilities were extracted from European call and put options written on the selected stocks from June 30, 2009 to April 30, 2017 with a one month maturity and with moneyness between 80% and 120%. As risk-free interest rate we take the Euribor rate. Since we considered dividend adjusted closing prices, we assumed that $d_j = 0$ for each stock j. By an empirical test it follows that under this assumption on dividends the put-call parity continues to be fulfilled.

[1] We select Unicredit Bank and Assicurazioni Generali instead of CRH and Engie.

4 Double calibration

In this Section we consider a calibration framework in which we jointly (1) estimate the model parameters on the multivariate time series of log-returns, by minimizing, for each margin, the Kolmogorov-Smirnov distance under the historical measure, and (2) calibrate the implied volatility surface, by minimizing the average relative percentage error (ARPE), under the risk-neutral measure. We refer to this method as *double calibration* (see Tassinari and Bianchi [2014] for a detailed description of the calibration approach). By following this approach, for each margin, both the implied volatility and log-return calibration-estimation errors are minimized: we find a set of parameters such that the model implied volatilities are as close as possible to the market implied volatilities and, at the same time, the theoretical univariate distribution of log-returns is as close as possible to the empirical distribution.

Specifically, on each trading day we estimate the model parameters by solving the following minimization problem

$$\widehat{\Theta}^Q = \min_{\Theta^Q} \Big(\sum_j \big(ARPE_j(\Theta^Q) + \xi_1 KS_j(\Theta^{P_h}) \big) \Big), \tag{4.1}$$

where

$$ARPE_j(\Theta^Q) = \frac{1}{\text{number of observations}} \sum_{T_n} \sum_{K_m} \frac{|iVol^{market}_{T_n K_m} - iVol^{model}_{T_n K_m}(\Theta^Q)|}{iVol^{market}_{T_n K_m}}, \tag{4.2}$$

in which $iVol^{market}_{T_n K_m}$ ($iVol^{model}_{T_n K_m}$) denotes the market (model) implied volatility of the option with maturity T_n and strike K_m, the index j represents the stock j, and Θ^Q is the vector of the risk neutral parameters. Furthermore, $KS_j(\Theta^{P_h})$ in (4.1) indicates the Kolmogorov-Smirnov distance associated to the j-th margin, given the set of parameters Θ^{P_h} derived from the risk-neutral parameters Θ^Q by means of the inverse Esscher transform. To perform the inverse Esscher transform, we solve the systems (2.13) and (2.22) in the MNTS and in the MGH model, respectively. As done in Tassinari and Bianchi [2014], ξ_1 is fixed to 3. Additionally, the algorithm is implemented by following the pricing method for standard vanilla options proposed in Carr and Madan [1999] and the expectation-maximization (EM) maximum likelihood estimation method as described in Tassinari and Bianchi [2014] and Bianchi et al. [2016]. We point out that the matrix A, representing the lower triangular Cholesky factor of the matrix Ω, is estimated through the EM-based maximum likelihood method before running the double calibration approach and it is kept fixed in the optimization algorithm. Therefore, all model parameters may change during the optimization procedure except for the elements of the correlation matrix of the underlying Brownian motion. However, we want to emphasize that this in no way implies the constancy of log-returns correlations during the optimization phase of the double-calibration (see (2.9) and (2.18)). For further technical and computational details on the double calibration approach see Tassinari and Bianchi [2014]. A detailed error analysis of the EM-based ML estimation method for the MNTS and MGH random variables has been conducted in Bianchi et al. [2016]. The double calibration approach is more robust since at each step considers also option implied data. The calibration conducted using only option implied data may be problematic. Here the numerical errors are controlled by construction (see also Chapter 11 in Bianchi et al. [2019]). We start with the historical estimation and jointly minimize the objective function in equation (4.1).

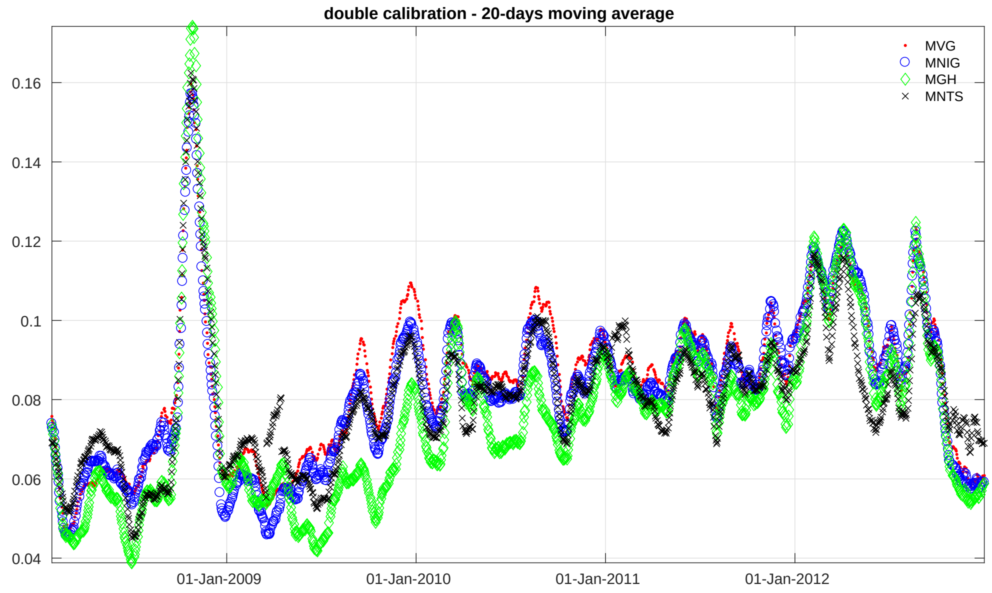

Figure 1: Implied volatility calibration error (ARPE) for all stocks and models analyzed under the double calibration approach (20-day moving average). The calibration was conducted on a daily basis for each trading day between January 2, 2008 to December 31, 2012.

4.1 Comparison with the MNIG and the MVG model

In this section we compare the calibration errors of the MGH and of the MNTS models with those reported in Tassinari and Bianchi [2014], that is, with the multivariate Gaussian, the multivariate variance gamma (MVG) and the multivariate normal inverse Gaussian (MNIG) models. Based on the ARPE evaluated over the entire sample on successive cross-sections of implied volatilities and stocks, the MGH model shows a smaller calibration error in fitting implied volatilities. The error is larger for IBM (in median, 9.25 per cent in MGH model, and 10.20 per cent in the MNTS model) and smaller for Dell (in median, 6.40 per cent in the MGH model, and 6.50 per cent in the MNTS model). The time series of the ARPE computed across all five stocks simultaneously ranges from 3.16 per cent to 21.38 per cent (in median, 7.18 per cent) for the MGH model, and from 3.34 per cent to 32.71 per cent (in median, 7.74 per cent) for the MNTS model.

On October 17, 2008 (March 19, 2009) the MGH (MNTS) model reaches the largest calibration error. As already observed in Guillaume [2012], multivariate models based on Lévy processes performed badly during the crisis period. In Figure 1 we report the time series of the 20-days moving average of the median ARPE computed across all five stocks, for both the MGH model and the MNTS one, and compare them with the MNIG and MVG models analyzed in Tassinari and Bianchi [2014]. For each stock and for each model we evaluate the ARPE over the entire period. The 20-days moving average ranges from 3.88 per cent and 17.42 per cent (on average, 7.61 per cent) in the MGH case, from 4.51 per cent and 16.24 per cent (on average, 8.05 per cent) in the MNTS case, from 4.54 per cent and 15.72 per cent (on average, 8.18 per cent) in the MNIG case, and from 4.71 per cent and 15.97 per cent (on average, 8.47 per cent) in the MVG case. As expected

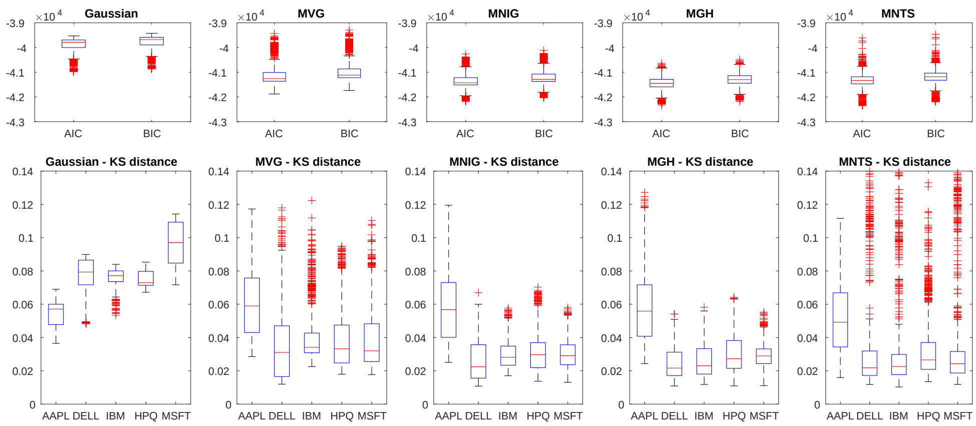

Figure 2: Goodness of fit statistics of the models estimated using the double calibration approach for each trading day from January 2, 2008 to December 31, 2012. For each trading day, a window of fixed size is considered (1,500 trading days) for a total of 1,259 rolling windows estimations for each model. For each model the boxplots of the AIC, the BIC and the univariate KS distance are reported. On each boxplot, the central mark is the median, the edges of the box are the 25-*th* and 75-*th* percentiles, the whiskers extend to the most extreme data points not considered outliers, and outliers are plotted individually.

the MGH model has a smaller average implied volatility calibration error than both the MNIG and the MVG model. The MNTS model has also a slightly better performance compared with both the MNIG model and the MVG one. Additionally, by considering similar studies on this subject (see Bianchi et al. [2018]), the implied volatility calibration error, for the MGH and the MNTS models, is satisfactory.

After having analyzed the implied volatility calibration error, we study the ability in fitting time series of log-returns of the MGH and the MNTS models and compare their performace with that of the MNIG and the MVG models analyzed in Tassinari and Bianchi [2014]. For all calibrated models, in Figure 2 we report the boxplot of both the Akaike information criterion (AIC) and the Bayesian information criterion (BIC). According to both the AIC and the BIC, the MGH is the best performing model and the Gaussian is the worst one. We point out that we conducted a maximum likelihood estimation for Gaussian model, without computing the corresponding implied volatility calibration error. Additionally, Figure 2 shows the boxplots of the KS statistic for each margin. The average p-value ranges from 2.34 (APPL) to 45.79 (DELL) per cent in the MGH model, and from 5.51 (APPL) and 43.46 (DELL) per cent in the MNTS model.

We remind that the historical parameters Θ^{P_h} are computed through the inverse Esscher transform. Except for Apple and, particularly for the MNTS model, the KS statistics are smaller compared to the KS statistics computed under the multivariate normal assumption. As shown in Figure 2, the MNIG and the MVG models exhibit a worst performance than both the MGH and MNTS model. The average p-value ranges from 1.59 (APPL) to 45.19 (DELL) per cent in the MNIG model, and from 0.88 (APPL) and 35.48 (DELL) per cent in the MVG model. While the MGH model outperforms its competitor models in calibrating the volatility surface, the MNTS model is slightly better in explaining the behaviour of time series of log-returns, at least for the data considered in

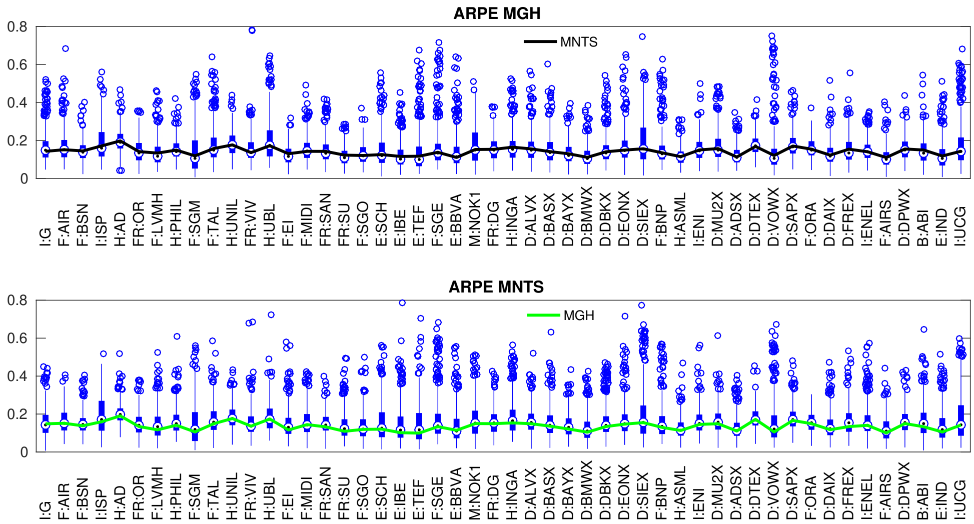

Figure 3: Implied volatility calibration error (ARPE) for each stock and each model analyzed under the double calibration approach (boxplot). For each stock the boxplot of the ARPE of a given model is compared to the median values of the ARPE of the competitor models. The calibration was conducted on a weekly basis for each Wednesday between June 30, 2009 to April 31, 2017.

this section. In Section 5 we further analyze these models in a portfolio selection exercise.

Finally, to perform a double calibration on a given trading day, that is to calibrate the five observed volatility surfaces and simultaneously estimate the five time series of log-returns, the computing time is, in median, 90 seconds in the MNIG case, and 190 seconds in the MVG case. The computing time for both the MGH and the MNTS model is larger (respectively, 200 and 400 seconds). This procedure was run on an 8 cores AMD FX 8120 processor with 16GB of Ram with a Linux based 64-bit operating system. Most of the computing time is spent on the optimization part of the code. The optimization algorithm applied in this study is a sequential quadratic programming method implemented in the *fmincon* Matlab function in which the option *active-set* is selected with the *UseParallel* option always switched on (i.e. the optimization function makes use of the Matlab Parallel toolbox).

In the optimization algorithm, we constrain the three MGH parameters (λ, χ, ψ) in the region between (-4.5, 1e-2, 1e-2) and (-0.5, 5, 2), and the three MNTS parameters (α, λ, C) in the region between (0.75, 1e-2, 1e-2) and (1.75, 5, 100). While in the MGH (MNTS) case the parameter σ_j ranges between 0.01 and 0.15 (0.01 and 0.2), θ_j ranges between -0.1 and 0.01 (-0.15 and 0.01).

4.2 A large scale empirical test

For further empirical investigation, we apply the calibration described in Section 4 to a large scale case. That is, we assess the double calibration approach to fit both the MGH and the MNTS model on all Euro denominated stocks included in the EuroStoxx 50 and we compare them with the multivariate Gaussian model with parameters μ and Σ. As usual, μ represents the annualized mean vector and Σ is the annualized variance-

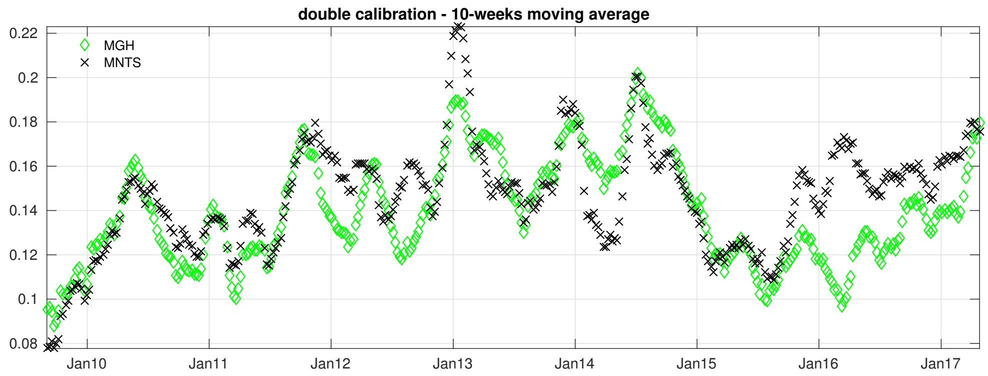

Figure 4: Implied volatility calibration error (ARPE) for all stocks and models analyzed under the double calibration approach (10-weeks moving average). The calibration was conducted on a weekly basis for each Wednesday between June 30, 2009 to April 31, 2017.

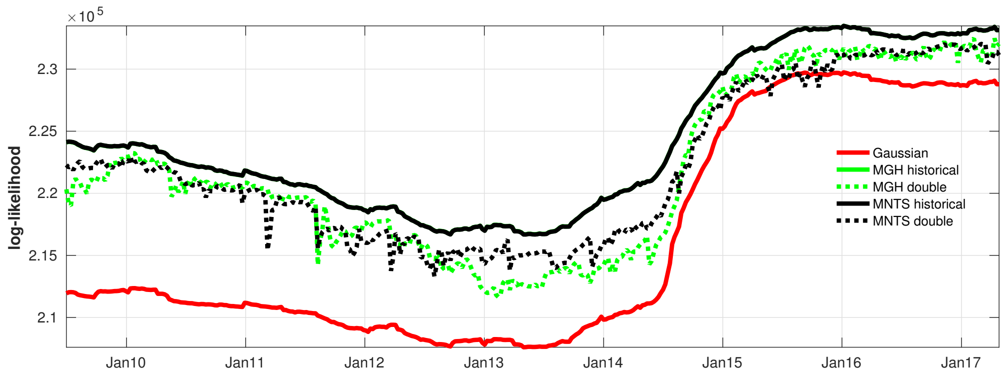

Figure 5: Log-likelihood of the models estimated using the historical and the double calibration approach for each Wednesday from June 30, 2009 to April 31, 2017. For each trading day, a window of fixed size is considered (1,500 trading days) for a total of 409 rolling windows estimations for each model.

covariance matrix. Both parameters are calibrated only to the time series of stock log-returns. We point out that the two non-Gaussian models have 53 more parameters compared to the Gaussian model, that is, the three parameters of the subordinator and the 50-dimensional vector θ.

The calibration is conducted for each Wednesday from June 30, 2009 to April 31, 2017. For each Wednesday, a window of fixed size is considered (1,500 daily observations) for a total of 409 rolling windows estimations for each model. The models are fitted on these time series of stock log-returns and to the 50 one-month implied volatility smiles observed at each given Wednesday. While in Section 4.1 we calibrate the models to the entire volatility surface, here we consider only the one-month maturity implied volatility smile.

Based on the ARPE evaluated over the entire sample of implied volatilities and stocks, the MGH model shows a smaller calibration error in fitting implied volatilities, as shown in Figure 3, in which the boxplots of the ARPE computed across the 409 rolling windows are reported. While in the MGH case the median error ranges from 9.95 (Telefonica -

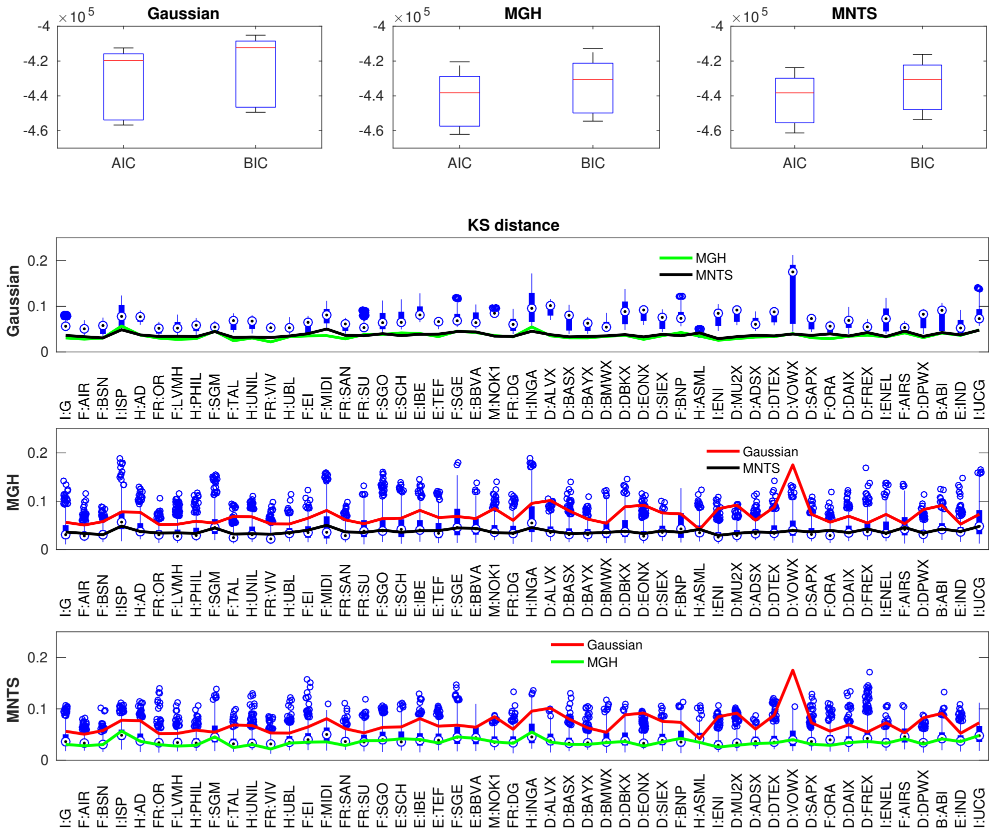

Figure 6: Goodness of fit statistics of the models estimated using the double calibration approach for each Wednesday from June 30, 2009 to April 31, 2017. For each trading day, a window of fixed size is considered (1,500 trading days) for a total of 409 rolling windows estimations for each model. For each model the boxplots of the AIC, the BIC and the univariate KS distance are reported. For each stock the boxplot of the KS distance of a given model is compared to the median values of the KS distance of the competitor models. On each boxplot, the central mark is the median, the edges of the box are the 25-*th* and 75-*th* percentiles, the vertical line extend to the most extreme data points not considered outliers, and outliers are plotted individually.

E:TEF) to 19.03 (Ahold Delhaize - H:AD) per cent, in the MNTS case it ranges from 10.99 (Airbus - F:AIRS) to 19.76 (Ahold Delhaize - H:AD) per cent. In 8 cases over 50 the median calibration error of the MNTS model is smaller compared to the error of the MGH model.

As shown in Figure 4, the time series (10-weeks moving average) of the median ARPE computed across all 50 stocks ranges from 8.80 per cent to 20.20 per cent (on average, 13.94 per cent) for the MGH model, and from 7.77 per cent to 22.30 per cent (on average, 14.64 per cent) for the MNTS model.

In Figure 5 we report the time series of the log-likelihood for all competitor models and estimation methods. The maximum likelihood estimation is considered in the normal case, the EM-based maximum likelihood estimation method in the MGH historical and MNTS historical cases, the double calibration approach is applied in the MGH double and MNTS double cases. Even if the double calibration approach is not focused on maximizing the likelihood, there are only few days when the log-likelihood of the MNTS model is smaller that the likelihood of the normal model (the log-likelihood of the MGH model is never smaller). This shows the great flexibility of the MGH and MNTS models with respect to the normal one: they are able to jointly calibrated log-returns and implied volatility smile and their log-likelihood is still greater than the estimated log-likelihood under the normal framework. As expected, in both MGH and MNTS cases, the log-likelihood of the models estimated by considering only historical information is larger. The log-likelihoods of MGH historical and MNTS historical are almost indistinguishable.

As far as the double calibration is concerned, according to both the AIC and the BIC, the MNTS model is better because its AIC and BIC average values are smaller compared with all other competitor models, and the Gaussian one is the worst (see Figure 6). Additionally, Figure 6 shows the boxplots of the KS statistic for each margin. In 18 cases over 50 the calibration error (average values) of the MNTS model is smaller compared to the error of the MGH one. For all stocks and for both the MGH and the MNTS model, the KS statistic is smaller compared to that of the Gaussian model. The p-value (average value) is bigger than 5 per cent in 44 cases over 50 for the MNTS model, in 49 cases for the MGH model and never for the Gaussian one.

Finally, to perform a double calibration on a given Wednesday, that is to calibrate the 50 observed volatility surfaces, and simultaneously estimate the time series of log-returns, the computing time is, in median, 350 seconds in the MGH case, and 1,350 seconds in the MNTS case. The procedure is run on the same machine and with the same implementation described in Section 4.1.

5 A portfolio selection analysis

In this section we provide the necessary definitions needed to implement a minimum-AVaR portfolio selection criterion and show the backtest of a portfolio selection strategy applied to the 50-dimensional case investigated in Section 4.2.

The value at risk (VaR) of a continuous random variable X, representing the profit-and-loss or the return of a portfolio, at tail probability level δ is

$$VaR_\delta(X) = -\inf\{x|P(X \leq x) > \delta\} = -F_X^{-1}(\delta)$$

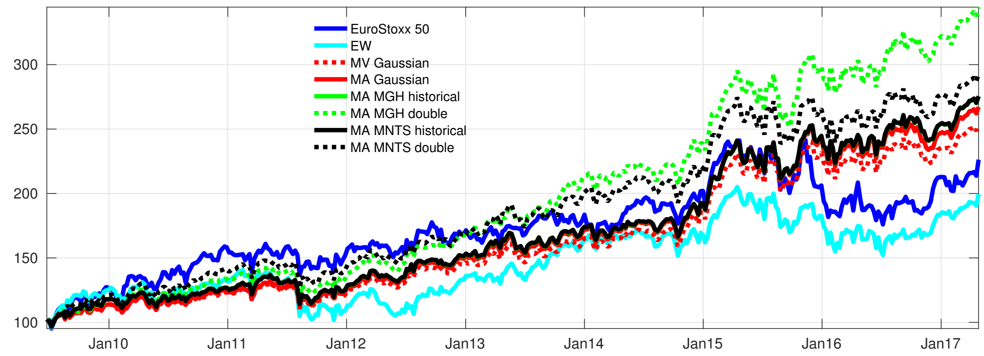

Figure 7: Portfolio selection backtest with weekly rebalacing for each Wednesday from June 30, 2009 to April 31, 2017 (for a total of 409 rebalancing days) for the MV, EW and MA strategies. The resulting portfolio values are scaled to 100 for the first date of the backtest period. For the MGH and the MNTS both the historical and the double calibration approaches are considered to find the MA weights.

and it can be computed by inverting the cumulative distribution function F_X. The AVaR of a continuous random variable X with finite mean (i.e. $E[X] < \infty$) at tail level δ is the average of the VaRs that are greater than the VaR at the same tail level, that is

$$AVaR_\delta(X) = \frac{1}{\delta}\int_0^\delta VaR_p(X)dp = -E\big[X\big|X < -VaR_\delta(X)\big].$$

Thus, the AVaR measures the expected loss, given that the loss has exceeded the VaR at the same probability level. We refer to $VaR_{0.05}(X)$ and $AVaR_{0.05}(X)$ as *5% VaR* and *5% AVaR*, respectively.

By considering the result of Proposition 1 in Kim et al. [2012] (see also Bianchi et al. [2016]), it follows that if $Y = \{Y_t, t \geq 0\}$ is a MNTS process, $Y_{\Delta t}$ is the distribution of its increments with discrete time step Δt, and $w \in \mathbb{R}^n$, then $w'Y_{\Delta t}$ is a univariate NTS random variable with characteristic function

$$\Psi_{w'Y_{\Delta t}}(v) = \exp\left\{\Delta t\left[iv\tilde{\mu} + C\Gamma(-\alpha)\left(\left(\lambda - iv\tilde{\theta} + \frac{1}{2}v^2\tilde{\sigma}^2\right)^\alpha - \lambda^\alpha\right)\right]\right\}, \qquad (5.1)$$

where

$$\tilde{\theta} = w'\theta, \qquad \tilde{\mu} = w'\mu, \qquad \tilde{\sigma} = \sqrt{w'\Sigma w}.$$

This means that a portfolio of margins with joint MNTS distribution is a NTS random variable. This property is very useful for computing portfolio risk measures, since it reduces the dimension of the problem from n to 1 and the portfolio distribution belongs to the same parametric family. Furthermore, from Kim et al. [2010b] and Kim et al. [2011] it is possible to obtain a closed formula (up to an integration) to compute the average value at risk (AVaR) in the NTS case. Since it is a standard practice in the industry to consider VaR and AVaR as positive numbers to be converted in capital requirements for trading book positions, we consider the formulas of Kim et al. [2010b] changed by sign. In the MGH case, the VaR and AVaR computation is simpler, since a portfolio of MGH margins is a GH random variable and a closed-form expression for the density function can be used. In the normal case, the VaR and the AVaR can be easily evaluated.

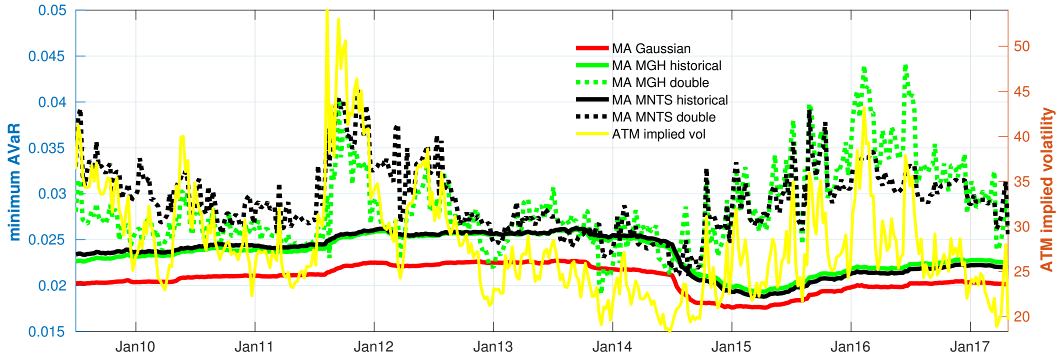

Figure 8: AVaR estimates for the MA portfolio strategy with weekly rebalacing for each Wednesday from June 30, 2009 to April 31, 2017 (for a total of 409 rebalancing days). For the MGH and the MNTS both the historical and the double calibration approach are considered to find the MA weights.

The portfolio selection strategy proposed here is based on the minimum-AVaR (MA) approach. Given a distributional assumption, we find the weights minimizing the AVaR (see Stoyanov et al. [2010]) at a given tail level. We suppose that short selling is not allowed and that it is not possible to invest more than 10% of the wealth in a specific stock (i.e. $0 \leq w_j \leq 0.1$). Then, we consider $\delta = 0.05$. Due to the convexity property of AVaR, the problem has a unique minimum which can be obtained through the standard first-order optimality conditions for constrained optimization problems. We apply this approach to the Gaussian, the MGH and the MNTS models. In the non-Gaussian cases we consider both the historical and the double calibration approach. The former calibration is based on the time-series of stock log-returns only, for this reason we refer to it as *historical*. As described in Section 4, the latter uses both time-series of stock log-returns and option implied volatility, and we refer to it as *double*.

The performance of the proposed long-only strategy is benchmarked against the minimum-variance (MV) portfolio and the equally weighted (EW) portfolio with rebalancing. These fundamental strategies are important benchmarks for large-scale applications. As done in Mainik et al. [2015], the comparison includes annualized portfolio returns, maximum drawdowns, transaction costs, portfolio concentration, and asset diversity in the portfolio. Note that none of the three compared methods (MV, EW, and MA) looks at expected returns.

The analysis is based on the estimates described in Section 4.2. The computation of portfolio weights utilizes the estimates based on the time series of stock log-returns from the six years prior to each Wednesday and the one-month implied volatility smile observed on that Wednesday. For example, the optimal portfolio for July 1, 2009 is estimated from the stock price data for the period from July 2, 2003 to July 1, 2009 and the one-month implied volatilities observed on July 1, 2009. While the estimates are based on daily data, the rebalancing is performed on a weekly basis. Estimating both the MGH and the MNTS model on each trading day is too time-consuming for our computing resources. As observed in Section 4.2, for each estimation day, it needs around half an hour to calibrate the two non-Gaussian models (MGH and MNTS).

In Figure 7 we report the behavior of the total wealth for all strategies and for the

	TR	AR	Sharpe	MaxDD	CC	PT	Z_1	Z_2
EuroStoxx 50	81.6%	10.4%	7.2%	27.1%	-	-	-	-
EW	69.1%	8.8%	5.9%	27.7%	50.0	0.0202	-	-
MV normal	93.0%	11.8%	10.7%	15.8%	12.3	0.0161	-	-
MA normal	98.3%	12.5%	11.3%	15.2%	12.4	0.0160	0.0004	0.4322
MA MGH historical	101.3%	12.9%	11.6%	16.6%	12.1	0.0157	0.3459	0.5249
MA MGH double	123.7%	15.7%	14.1%	16.1%	11.8	0.0162	0.7677	0.9814
MA MNTS historical	101.3%	12.9%	11.6%	16.6%	12.2	0.0157	0.4201	0.5743
MA MNTS double	107.5%	13.7%	12.3%	14.5%	11.8	0.0158	0.8978	0.9847

Table 1: Portfolio selection backtest with weekly rebalacing for each Wednesday from June 30, 2009 to April 31, 2017 (for a total of 409 rebalancing days) for the MV, EW and MA strategies. We consider the following performance measures: total return (TR), annualized return (AR), Sharpe ratio (Sharpe), maximal drawdown (MaxDD), concentration index (CC) and portfolio turnover (PT). The AVaR is computed by considering a 5% tail level. The p-values of the AVaR back-tests proposed by Acerbi and Székely [2014] are also reported.

EuroStoxx 50 index. The estimated optimal AVaR of the MA strategy applied to different distributional assumptions (Gaussian, MGH and MNTS) and estimation methods (historical and double) is reported in Figure 8. The dynamics of the AVaR are compared with the at-the-money (ATM) implied volatility. By construction the optimal AVaR obtained by considering MGH and MNTS estimates based on the double calibration approach is more volatile. Note that the double calibration approach takes into consideration the behavior of the implied volatility, that is usually less smooth than the historical one.

In Table 1 we show the results of the MA approach compared to its competitor strategies and to the EuroStoxx 50 index. We report the total return (TR) over the observation period, the corresponding annualized return (AR), the Sharpe ratio, the maximum drawdown (MaxDD), the concentration coefficient (CC) and the portfolio turnover (PT).

The TR is the logarithmic return over the entire observation period, and the AR is the TR divided by the number of years, that is 409 over 52 weeks. The Sharpe ratio is estimated on the portfolio returns over the observation period (409 weeks). To measure the portfolio stock concentration, we compute the concentration coefficient (CC) defined in Mainik et al. [2015] as

$$CC_t = \left(\sum_{j=1}^{n} \left(w_t^j \right)^2 \right)^{-1},$$

where w_t^j is the portion of portfolio wealth invested in the j-th stock at time t. The CC of an equally weighted portfolio is the number of assets n. As the portfolio becomes concentrated on fewer assets, the CC decreases.

As a proxy for transaction costs, we consider the portfolio turnover (PT) defined as

$$PT_t = \sum_{j=1}^{n} |w_t^j - w_{t_-}^j|,$$

where w_t^j is the portfolio weight of the asset j after rebalancing (according to the portfolio selection strategy) at time t, and $w_{t_-}^j$ is the portfolio weight of the asset j just before rebalancing.

The results show that the MA strategy indeed outperforms MV and EW portfolios in many respects. In particular, the MA optimal portfolio gives higher total returns, higher Sharpe ratios, and lower maximal drawdowns. Furthermore, the use of the information content of the implied volatility largely improve the portfolio performance. The strategies where the parameters are estimated with the double calibration approach outperforms all competitor strategies.

The best performer is the MA MGH double portfolio with the highest returns (15.7 per cent on an annual basis) and the highest Sharpe ratio (14.1 per cent). The overperformance on a yearly basis with respect to the EuroStoxx 50 index is 5.3 (3.3) per cent in the MA MGH (MNTS) double case, 2.5 per cent in the MA MNTS (MGH) historical case, 2.1 per cent in the MA Gaussian case and 1.4 in the MV Gaussian case. The EW strategy underperforms the EuroStoxx 50 index. The lowest maximal drawdown is obtained for the MA MNTS strategy (14.5 per cent), even if the value obtained for the MA normal strategy is quite close (15.2 per cent). It is slightly higher in the other non-Gaussian MA cases: it ranges from 16.1 to 16.6 per cent.

The results in Table 1 indicate that the MA and the MV strategies are quite selective, whereas the number of stocks in the MA portfolio under the double calibration approach is slightly smaller. The average turnover of MA optimal portfolios ranges from 0.0157 to 0.162 and it is close to that of the MV portfolio (0.0161). Surprisingly the EW strategy shows the highest PT (0.0202).

For all proposed strategies involving AVaR minimization, we back-test the portfolio AVaR model as suggested by Acerbi and Székely [2014]. In particular, the last two columns of Table 1 contain the p-value of the test 1 and the test 2 of Acerbi and Székely [2014], to which we refer to as Z_1 and Z_2. While test 2 allows to accept all AVaR models, test 1 rejects only the normal one. To compute the p-values we simulated 10,000 random variates for each time t. As shown in Table 1, the p-value varies accross different models and calibration approaches. Before performing test 1, we conducted a preliminary VaR back-test as proposed by Christoffersen [2010]. In all cases the VaR models show a good performance.

As a further empirical investigation, we switch from weekly to monthly (four weeks), quarterly (13 weeks), semi-annually (26 weeks), annually (52 weeks), biennially (104 weeks), quadrennially (208 weeks) rebalancing and the buy-and-hold (no rebalacing over the entire observation period). The calculation of portfolio weights is still based on the estimates provided in Section 4.2. This allows using all observations in the historical window, and not only a subset. The Sharpe ratio is estimated on the portfolio returns over the observation period (409 weeks). Both the AR and the Sharpe ratios are reported in Figure 9. While for the strategies based only on historical information, the performance decreases if one decreases the rebalacing frequency, for both strategies that use also the implied volatility information, the performance seems to be less affected by the rebalancing frequency.

As robustness check, we perform a portfolio selection strategy in which the expected return is maximized subject to a constraint on the AVaR. It is well established that investors typically maximize portfolio expected returns subject to a constraint on the amount of risk. We refer to this strategy as MR. Four different amounts of risk are tested: 1.5, 2, 2.5 and 3 per cent (in the optimization algorithm we constrain the AVaR to be less or equal to the given amount of risk).

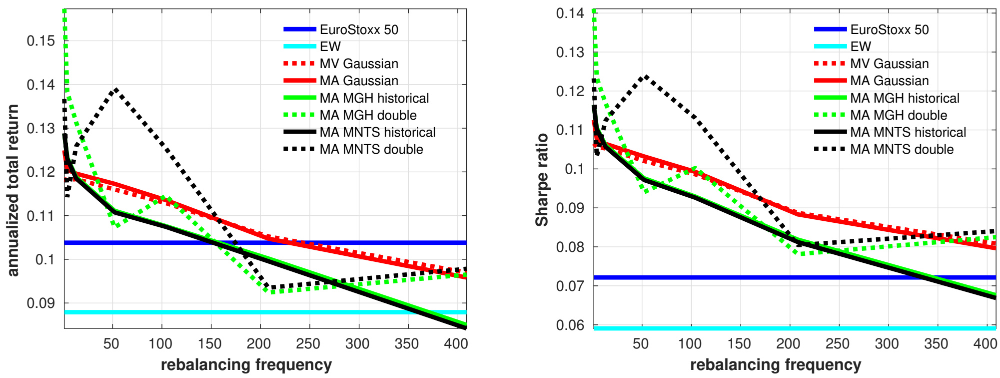

Figure 9: For each model we compare the portfolio strategy performance by switching from weekly to monthly (four weeks), quarterly (13 weeks), semi-annually (26 weeks), annually (52 weeks), biennially (104 weeks), quadrennially (208 weeks) rebalancing and the buy-and-hold (no rebalacing over the entire observation period). Total annualized returns and Sharpe ratios are reported.

	TR	AR	Sharpe	MaxDD	CC	PT	Z_1	Z_2
EuroStoxx 50	81.6%	10.4%	7.2%	27.1%	-	-	-	-
			1.5%					
MR normal	76.1%	9.7%	11.6%	11.0%	18.4	0.2603	0.0013	0.2756
MR MGH historical	68.5%	8.7%	11.9%	10.2%	22.9	0.3525	0.2104	0.5757
MR MGH double	78.5%	10.0%	17.3%	9.6%	29.2	0.4551	0.9405	0.9524
MR MNTS historical	69.6%	8.8%	11.9%	10.2%	22.8	0.3441	0.2742	0.6085
MR MNTS double	64.3%	8.2%	14.6%	6.7%	29.9	0.4663	0.9574	0.9321
			2%					
MR normal	99.3%	12.6%	11.5%	14.4%	13.3	0.0510	0.0033	0.2859
MR MGH historical	89.8%	11.4%	11.7%	13.6%	15.3	0.1410	0.2760	0.5646
MR MGH double	99.2%	12.6%	16.3%	12.6%	18.6	0.2700	0.9235	0.9745
MR MNTS historical	90.8%	11.5%	11.7%	13.5%	15.6	0.1401	0.4109	0.5725
MR MNTS double	79.6%	10.1%	13.6%	9.0%	19.6	0.2919	0.9353	0.9795
			2.5%					
MR normal	130.3%	16.6%	13.0%	18.2%	14.2	0.0178	0.0001	0.5791
MR MGH historical	108.7%	13.8%	11.6%	17.0%	13.2	0.0204	0.2285	0.4911
MR MGH double	109.4%	13.9%	14.4%	16.0%	14.2	0.1060	0.7975	0.9915
MR MNTS historical	110.5%	14.0%	11.8%	16.9%	13.2	0.0216	0.4155	0.4854
MR MNTS double	97.1%	12.3%	13.5%	11.6%	15.1	0.1346	0.9361	0.9514
			3%					
MR normal	150.1%	19.1%	14.3%	18.5%	13.0	0.0179	0.0005	0.3396
MR MGH historical	140.0%	17.8%	13.6%	18.2%	13.1	0.0177	0.1776	0.3781
MR MGH double	106.3%	13.5%	12.4%	19.9%	14.7	0.0377	0.7639	0.9842
MR MNTS historical	146.0%	18.6%	14.2%	18.4%	12.8	0.0178	0.1995	0.4800
MR MNTS double	98.5%	12.5%	11.7%	16.2%	14.6	0.0403	0.8579	0.8601

Table 2: Portfolio selection backtest with weekly rebalacing for each Wednesday from June 30, 2009 to April 31, 2017 (for a total of 409 rebalancing days) for the MR strategies with the constraint on the maximum amount of risk (i.e. 1.5%, 2%, 2.5% and 3%). We consider the following performance measures: total return (TR), annualized return (AR), Sharpe ratio (Sharpe), maximal drawdown (MaxDD), concentration index (CC) and portfolio turnover (PT). The AVaR is computed by considering a 5% tail level. The p-values of the AVaR back-tests proposed by Acerbi and Székely [2014] are also reported.

The results are reported in Table 2. As expected, total returns increase as the amount of risk increases. Even if the MR strategy is not always able to overperform the EuroStoxx 50, it has a better Sharpe ratio. At an amount of risk corresponding to a maximum AVaR of 1.5 per cent, the best performance in terms of total return among the MR strategies is reached by the MR MGH double portfolio with a 10 per cent annualized return. For higher amounts of risk, the MR normal portfolios exhibit higher total returns, with an annualized return of 12.6 per cent for a maximum AVaR of 2 per cent, 16.6 per cent for a maximum AVaR of 2.5 per cent, and 19.1 per cent for a maximum AVaR of 3 per cent. Conversely, the worst results in terms of total return are achieved by the MR MNTS double portfolios for all four levels of risk. However, a further inspection of Table 2 reveals that both MR double portfolios have better performances in terms of Sharpe ratios for the three lowest levels of risk considered. As we move from the lowest to the highest AVaR level, the over-performances in terms of Sharpe ratios of the MR MGH (MNTS) double model with respect to the EuroStoxx 50 index are 10.1 (7.4), 9.1 (6.4), 7.2 (6.3), and 5.2 (4.5) per cent. Notice that as the AVaR level increases the over-performance of the MR double portfolios in terms of Sharpe ratio decreases. When the maximum amount of risk is 3 per cent, MR double portfolios have the worst performance. All MR portfolios have lower maximal drawdown compared to the EuroStoxx 50 index and all maxima drawdowns increase as the portfolio risk rises. In all four cases the MR MNTS double portfolios have the lowest maximal drawdowns and, for the three smallest AVaR level (i.e. 1.5, 2, 2.5 per cent), the MR MGH double portfolios are the second best in terms of MaxDD. We observe also that both MR double strategies lead to portfolios with higher CC and PT indexes and that their value decreases as we increase the AVaR. In the last two columns of Table 2 the *p*-values of the AVaR back-tests Z_1 and Z_2 are reported. The first test rejects only the normal AVaR model while the second one refuses none.

As far as the optimization algorithm is concerned, it should be noted that when the amount of risk is high (i.e. 3 per cent), the upper bound of the AVaR constraint is not always reached. Additionally, the optimization algorithm based on MA seems to be more stable compared to the MR one. As observed in Bianchi et al. [2019] and reference therein, in portfolio construction there is the issue of the sensitivity to mention. This phenomenon was studied by Merton [1980], who among others argued that the estimates of the variances and the covariances of the asset returns are more accurate than the estimates of the means. Best and Grauer [1991] showed that the sample efficient portfolio is extremely sensitive to changes in the asset means. Chopra and Ziemba [1993] concluded for a real data set that errors in means are over 10 times as damaging as errors in variances and over 20 times as errors in covariances. For this reason many authors do not consider asset expected returns and choose portfolio weights by minimizing a given risk measure.

6 Conclusion

The objective of this paper is threefold. First, we propose a multivariate option pricing framework based on heavy tails, negative skewness and asymmetric dependence. The connection between the historical measure and the risk-neutral measure is given by the Esscher transform. This link allows one to take into account simultaneously both multivariate time-series of log-returns and implied volatility smiles.

Second, we conduct a large scale empirical study based on a joint calibration-estimation of the univariate option surfaces time series of log-returns has been proposed. The model is calibrated without the need of multivariate derivative quotes. The EM-based maximum likelihood estimation method is applied to have a first estimate of the historical parameters. Thus, we jointly estimate the model parameters on the time series of log-returns by minimizing (1) the average relative percentage error, which is a measure of the distance between model and observed implied volatilities, and (2) the Kolmogorov-Smirnov distance between the theoretical and empirical historical distributions. The historical measure and the risk-neutral one are connected through the Esscher transform.

Third, we show how to use the proposed framework to evaluate portfolio risk measures. The models analyzed allow for a quasi-closed form solution for the evaluation of both VaR and AVaR. Forecasts of risk measures for portfolios of assets can be obtained in a computationally straightforward manner and the model can be cast into a portfolio optimization algorithm to efficiently solve a portfolio selection problem. We empirically assess the importance of considering the information coming from implied volatility smiles under a minimum-risk portfolio selection strategy with multivariate non-Gaussian distributions.

The jumps allowed in both the NTS and the GH model may cause that during the day, especially for complex trading positions, the portfolio losses exceed a specified level and then at the end of the day the portfolio value increases back. For this reason Bakshi, G. and Panayotov, G. [2010] suggested the intra-horizon VaR (VaR-I). Unlike the VaR and the AVaR measure, VaR-I reflects the magnitude of losses within a trading horizon, and not just at the end of the horizon. The calibration technique proposed in this paper could be extended to the VaR-I. Currently, there are methods for fast computing VaR-I for Lévy models in the univariate case only (see Kudryavtsev and Levendorskii [2009] and Kudryavtsev [2016]).

Finally, the multivariate non-Gaussian models proposed in this work together with the double calibration approach can be used to explore the interdependencies in financial markets, not only for solving portfolio selection problems, but also as a statistical tool for financial stability purposes. This tool for dependence modeling does not only allow for an accurate analysis beyond the linear correlation matrix and the common multivariate Gaussian distribution, but it is also able to incorporate market expectations through the use of option implied volatilities.

References

C Acerbi and B. Székely. Back-testing expected shortfall. *Risk*, 27, 2014.

A. Anand, T. Li, T. Kurosaki, and Y.S. Kim. Foster–Hart optimal portfolios. *Journal of Banking & Finance*, 68:117–130, 2016.

Bakshi, G. and Panayotov, G. First-passage probability, jump models, and intra-horizon risk. *Journal of Financial Economics*, 95(1):20–40, 2010.

L. Ballotta and E. Bonfiglioli. Multivariate asset models using Lévy processes and applications. *The European Journal of Finance*, 22(13):1320–1350, 2016.

L. Ballotta, G. Deelstra, and G. Rayée. Multivariate FX models with jumps: Triangles, quantos and implied correlation. *European Journal of Operational Research*, 260(3): 1181–1199, 2017.

O.E. Barndorff-Nielsen. Processes of normal inverse Gaussian type. *Finance and Stochastics*, 2(1):41–68, 1997.

O.E. Barndorff-Nielsen and S.Z. Levendorskii. Feller processes of normal inverse gaussian type. *Quantitative Finance*, 1(3):318–331, 2001.

M.J. Best and R.R. Grauer. On the sensitivity of mean-variance-efficient portfolios to changes in asset means: some analytical and computational results. *Review of Financial Studies*, 4(2):315–342, 1991.

M.L. Bianchi. Are the log-returns of Italian open-end mutual funds normally distributed? A risk assessment. *Journal of Asset Management*, 16(7):437–449, 2015.

M.L. Bianchi, S.T. Rachev, Y.S. Kim, and F.J. Fabozzi. Tempered infinitely divisible distributions and processes. *SIAM Theory of Probability and Its Applications*, 55(1): 59–86, 2010.

M.L. Bianchi, G.L. Tassinari, and F.J. Fabozzi. Riding with the four horsemen and the multivariate normal tempered stable model. *International Journal of Theoretical and Applied Finance*, 19(4), 2016.

M.L. Bianchi, S.T. Rachev, and F.J. Fabozzi. Calibrating the Italian smile with time-varying volatility and heavy-tailed models. *Computational Economics*, 51:339–378, 2018.

M.L. Bianchi, S.V. Stoyanov, G.L. Tassinari, F.J. Fabozzi, and S.M. Focardi. *Handbook of heavy-tailed distributions in asset management and risk management*. World Scientific, 2019.

S.I. Boyarchenko and S.Z. Levendorskii. Option pricing for truncated Lévy processes. *International Journal of Theoretical and Applied Finance*, 3(03):549–552, 2000.

S.I. Boyarchenko and S.Z. Levendorskii. *Non-Gaussian Merton-Black-Scholes theory.* River Edge, New Jersey: World Scientific Publishing, 2002.

P. Carr and D. Madan. Option valuation using the fast Fourier transform. *Journal of Computational Finance*, 2(4):61–73, 1999.

P. Carr, H. Geman, D.B. Madan, and M. Yor. The fine structure of asset returns: An empirical investigation. *The Journal of Business*, 75(2):305–332, 2002.

P. Carr, H. Geman, D.B. Madan, and M. Yor. Self-decomposability and option pricing. *Mathematical finance*, 17(1):31–57, 2007.

S. Cecchetti and L. Sigalotti. Forward-looking robust portfolio selection. *Working Paper, Banca d'Italia*, no. 913, 2013.

V.K. Chopra and W.T. Ziemba. The effect of errors in means, variances, and covariances on optimal portfolio choice. *Journal of Portfolio Management*, 19(2):6–11, 1993.

P. Christoffersen. Backtesting. In *Encyclopedia of Quantitative Finance*. Wiley, 2010.

R. Cont and P. Tankov. *Financial modelling with jump processes*. Chapman & Hall/CRC, 2003.

V. DeMiguel, L. Garlappi, and R. Uppal. Optimal versus naive diversification: How inefficient is the 1/N portfolio strategy? *Review of Financial Studies*, 22(5):1915–1953, 2007.

V. DeMiguel, Y. Plyakha, R. Uppal, and G. Vilkov. Improving portfolio selection using option-implied volatility and skewness. *Journal of Financial and Quantitative Analysis*, 48(6):1813–1845, 2013.

Y. Dominicy, H. Ogata, and D. Veredas. Inference for vast dimensional elliptical distributions. *Computational Statistics*, 28(4):1853–1880, 2013.

E. Eberlein and U. Keller. Hyperbolic distributions in finance. *Bernoulli*, 1(3):288–299, 1995.

E. Eberlein, , and K. Prause. The generalized hyperbolic model: Financial derivatives and risk measures. In H. Geman, D. Madan, S.R. Pliska, and T. Vorst, editors, *Mathematical Finance, Bachelier Congress*, pages 245–267. Springer Berlin Heidelberg, 2002.

H.A. Fallahgoul, Y.S. Kim, and F.J. Fabozzi. Elliptical tempered stable distribution. *Quantitative Finance*, 16(7):1069–1087, 2016.

H.A. Fallahgoul, Y.S. Kim, F.J. Fabozzi, and J. Park. Quanto option pricing with Lévy models. 53(3):1279–1308, 2019.

G. Frahm. *Generalized elliptical distributions: theory and applications*. PhD thesis, Universität zu Köln, 2004.

H.U. Gerber and E.S. Shiu. Option pricing by Esscher transform. *Transactions of the Society of Actuaries*, 46:99–144, 1994.

M. Grabchak. *Tempered stable distributions: Stochastic models for multiscale processes*. Springer, Cham, 2016.

F. Guillaume. Sato two-factor models for multivariate option pricing. *Journal of Computational Finance*, 15(4):159–192, 2012.

F. Guillaume. The αVG model for multivariate asset pricing: calibration and extension. *Review of Derivatives Research*, 16(1):25–52, 2013.

M. Hellmich and S. Kassberger. Efficient and robust portfolio optimization in the multivariate generalized hyperbolic framework. *Quantitative Finance*, 11(10):1503–1516, 2011.

W. Hu. Calibration of multivariate generalized hyperbolic distributions using the EM algorithm, with applications in risk management, portfolio optimization and portfolio credit risk. *PhD thesis, Florida State University*, 2005.

W. Hu and A.N. Kercheval. Risk management with generalized hyperbolic distributions. In P. Locke, editor, *Proceedings of the Fourth IASTED International Conference on Financial Engineering and Applications*, pages 19–24. ACTA Press, 2007.

W. Hu and A.N. Kercheval. Portfolio optimization for student-t and skewed-t returns. *Quantitative Finance*, 10(1):91–105, 2010.

A. Kempf, O. Korn, and S. Saßning. Portfolio optimization using forward-looking information. *Review of Finance*, 19(1):467–490, 2015.

Y.S. Kim, S.T. Rachev, M.L. Bianchi, and F.J. Fabozzi. Tempered stable and tempered infinitely divisible GARCH models. *Journal of Banking and Finance*, 34(9):2096–2109, 2010a.

Y.S. Kim, S.T. Rachev, M.L. Bianchi, and F.J. Fabozzi. Computing VaR and AVaR in infinitely divisible distributions. *Probability and Mathematical Statistics*, 30(2):223–245, 2010b.

Y.S. Kim, S.T. Rachev, M.L. Bianchi, I. Mitov, and F.J. Fabozzi. Time series analysis for financial market meltdowns. *Journal of Banking & Finance*, 35(8):1879–1891, 2011.

Y.S. Kim, R. Giacometti, S.T. Rachev, F.J. Fabozzi, and D. Mignacca. Measuring financial risk and portfolio optimization with a non-Gaussian multivariate model. *Annals of Operations Research*, 201(1):325–343, 2012.

S. Kring, S.T. Rachev, M. Höchstötter, F.J. Fabozzi, and M.L. Bianchi. Multi-tail generalized elliptical distributions for asset returns. *The Econometrics Journal*, 12(2): 272–291, 2009.

O. Kudryavtsev. Advantages of the Laplace transform approach in pricing first touch digital options in Lévy-driven models. *Boletín de la Sociedad Matemática Mexicana*, 22(2):711–731, 2016.

O. Kudryavtsev and S.Z. Levendorskii. Fast and accurate pricing of barrier options under Lévy processes. *Finance and Stochastics*, 13(4):531–562, 2009.

E. Luciano and P. Semeraro. A generalized normal mean-variance mixture for return processes in finance. *International Journal of Theoretical and Applied Finance*, 13(3): 415–440, 2010.

E. Luciano, M. Marena, and P. Semeraro. Dependence calibration and portfolio fit with factor-based subordinators. *Quantitative Finance*, 16(7):1037–1052, 2016.

G. Mainik, G. Mitov, and L. Rüschendorf. Portfolio optimization for heavy-tailed assets: Extreme Risk Index vs. Markowitz. *Journal of Empirical Finance*, 32:115–134, 2015.

A. McNeil, R. Frey, and P. Embrechts. *Quantitative risk management: Concepts, techniques, and tools.* Princeton University Press, 2005.

R.C. Merton. On estimating the expected return on the market: An exploratory investigation. *Journal of Financial Economics*, 8(4):323–361, 1980.

K. Prause. *The generalized hyperbolic model: Estimation, financial derivatives, and risk measures.* PhD thesis, Universität Freiburg i. Br., Freiburg i. Br, 1999.

R.S. Protassov. EM-based maximum likelihood parameter estimation for multivariate generalized hyperbolic distributions with fixed λ. *Statistics and Computing*, 14(1): 67–77, 2004.

S.T. Rachev, S.V. Stoyanov, and F.J. Fabozzi. *Advanced stochastic models, risk assessment, and portfolio optimization: The ideal risk, uncertainty, and performance measures.* Wiley, 2008.

S.T. Rachev, Y.S. Kim, M.L. Bianchi, and F.J. Fabozzi. *Financial models with Lévy processes and volatility clustering.* Wiley, 2011.

J. Rosinski. Tempering stable processes. *Stochastic processes and their applications*, 117 (6):677–707, 2007.

K. Sato. *Lévy processes and infinitely divisible distributions.* Cambridge University Press, 1999.

W. Schoutens. *Lévy processes in finance: Pricing financial derivatives.* Wiley, 2003.

S.V. Stoyanov, B. Racheva-Iotova, S.T. Rachev, and F.J. Fabozzi. Stochastic models for risk estimation in volatile markets: A survey. *Annals of Operations Research*, 176(1): 293–309, 2010.

M. Taboga. Option-implied probability distributions: How reliable? How jagged? *International Review of Economics & Finance*, 45:453–469, 2016.

G.L. Tassinari and M.L. Bianchi. Calibrating the smile with multivariate time-changed Brownian motion and the Esscher transform. *International Journal of Theoretical and Applied Finance*, 17(4), 2014.

G.L. Tassinari and C. Corradi. Pricing equity and debt tranches of collateralized funds of hedge fund obligations: An approach based on stochastic time change and Esscher-transformed martingale measure. *Quantitative Finance*, 13(12):1991–2010, 2013.

G.L. Tassinari and C. Corradi. Valuation of collateralized funds of hedge fund obligations: A basket option pricing approach. In M. Corazza and C. Pizzi, editors, *Mathematical and Statistical Methods for Actuarial Sciences and Finance*, pages 277–288. Springer, Cham, 2014.

X. Zhou, D. Malioutov, F.J. Fabozzi, and S.T. Rachev. Smooth monotone covariance for elliptical distributions and applications in finance. *Quantitative Finance*, 14(9): 1555–1571, 2014.